One-Step Reductive Electrodeposition of MOF Film on Polymer Membrane

Sijie Xie, Xuan Zhang,* Xiaoyu Tan, Wei Zhang, Wei Guo, Ning Han, Zhenyu Zhou, Yinzhu Jiang, Ivo F. J. Vankelecom, and Jan Fransaer*

ABSTRACT: **Reductive electrodeposition is a technique for the preparation of substrate-supported MOF films but is generally incompatible with poorly or nonconductive substrates like polymers and suffers from the possible codeposition of metallic impurities. Here, we report a facile and inexpensive strategy that achieves one-step reductive electrodeposition of impurity-free MOF films (i.e., HKUST-1 film) on nonconducting poly(ether sulfone) (PES) membranes. Unlike previously reported reductive electrodeposition configurations, which only contain the electrode−electrolyte interface near the working electrode, there are two tandem interfaces in the proposed approach, namely, the electrode−membrane interface and the membrane−electrolyte interface. Owing to the counter-diffusion of ions across the polymer membrane, this strategy allows the generation of MOF units on the membrane−electrolyte interface, while the codeposition of metal happens on the other, resulting in the deposition of a pure MOF film on untreated polymer membranes. Importantly, thanks to the inherent "self-closing" ability of the proposed electrochemical approach, a compact polycrystalline HKUST-1 film supported on PES membrane was obtained under mild conditions, which exhibited a rejection of 98.7% for rose bengal in an aqueous solution with a permeance of 7.4 L m^{-2} h^{-1} bar^{-1}.**

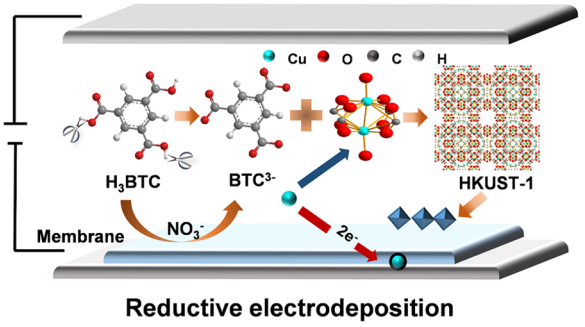

Metal−organic frameworks (MOFs), also known as porous coordination networks, have been studied for their porous nature and highly tunable physicochemical properties over the past decades.[1−10] Especially facing the rising demands on separation works like wastewater treatment and gas separations nowadays, extra attention has been paid to the MOF based separators since the MOFs with subnanosized apertures and high surface area are regarded as promising molecular sieves/adsorbents.[9,11] In most cases, the utilization of MOFs in separators involves mixed matrix membranes (MMMs) because of their high flexibility and easy scalability, which are prepared by mixing of the MOF powders and polymer matrices.[9,11] For example, Bene et al. integrated Zr-MOF nanoparticles into a polymer matrix and found that the obtained MOF contained MMM exhibited an outstanding performance on CO_2/CH_4 separation.[12] Deng and his colleagues reported the thickness-tunable Zn−MOF nanosheet contained MMMs for efficient CO_2/N_2 separation.[13] However, the MMMs could suffer from the inherent drawbacks of noncontinuous permeation pathways and the defects caused by the adverse interaction between MOF fillers and polymer matrices.[14,15] To this end, the in situ coating of MOF films on polymer membranes has been of interest recently because the MOF layer in a MOF-coated polymer membrane (MCPM) could act as an independent sieving medium.[11] For instance, Wang et al. reported a flexible ZIF-8 coated polypropylene (PP) membrane, which exhibited an impressive propene/propane separation performance without degradation by bending.[16] In the past few years, several techniques have been reported to fabricate MCPMs, for example, the seeded growth method,[17,18] layer-by-layer depositions,[19] microfluidic synthesis,[20] dip/spin coating methods,[21,22] evaporation induced method,[23] and chemical vapor deposition.[24] Nonetheless, these methods are either energy-consuming, complex, or slow, hampering their practical uses (Table S1).

Reductive electrodeposition is a technique for deposition of MOF films, first reported by Li and Dincă in 2011.[25] Given the simple operation process and mild conditions, this electrochemical technique is deemed a potential approach for the efficient and scalable fabrication of substrate supported MOF

films.[26] However, the reductive electrodeposition of flexible polymer membrane-supported MOF films is still in its infancy and yet greatly limited by some severe issues. For instance, the conductive working electrode (WE) is necessary to trigger the electrochemical reaction(s) in the electrodeposition process. Yet, the polymer membranes are generally of poor electric conductivity and not feasible to work as the WE directly. Even though a conductive layer coating strategy has been proposed by Lai et al. to mitigate this issue recently, it brings extra money, energy, and time costs for the additional Pt or carbon nanotube coating process.[27] Besides, on the basis of the theory proposed by Dincă et al., the reductive electrodeposition of MOF films relies on the negative bias induced deprotonation of linkers and the following coordination of the deprotonated linkers and the metal ions.[25,28] The undesirable metallic impurities could be cogenerated in the deposited MOF films due to the concurrent metal ions reduction along with the negative bias driven deprotonation of linkers. For example, Dincă et al. reported the metallic Zn impurities in the cathodically deposited MOF-5 (Zn-MOF) films, which was attributed to the much more negative applied potential (~1.73 V vs SHE) to trigger the deprotonation of H_2BDC (benzene-1,4-dicarboxylic acid) compared to the standard reduction potential of Zn^{2+} (−0.76 V vs SHE).[25] Notably, the codeposition of metal ions could even be more prominent when it comes to the reductive electrodeposition of MOFs with metal nodes that are more readily reduced than Zn^{2+}.[28,29] The codeposited nonporous metallic impurities impede the transport of the filter feed and create defects in the MOF film, such as cracks and voids, which are highly undesirable. Thus, it is very challenging to reductively electrodeposit impurity-free MOF films like the Zn-MOF and Cu-MOF films.

In this work, we report an easy and straightforward modification of the reductive electrodeposition to achieve the one-step preparation of pure MOF films (e.g., the HKUST-1 film and the Co-(HBTC)(4,4′-bipy) film) on polymer membranes under mild conditions. Unlike the conventional reductive electrodeposition of MOF films that only contains the WE−electrolyte interface, the proposed cathodic deposition has the WE−membrane and membrane−electrolyte interfaces, as shown in Figure 1. This strategy enables the reduction of the metal ion on the former interface, while the MOF film formation on the other, rendering the pure MOF coating on the polymer membrane. Moreover, owing to the "self-closing" ability of the electrochemical deposition, a compact HKUST-1 film comprised of closely packed MOF crystals was obtained on the poly(ether sulfone) (PES) membrane after a 16-h deposition at 323 K, which exhibited a 98.7% rejection of rose bengal in water with a permeance of 7.4 L m^{-2} h^{-1} bar^{-1}. The separation performance is comparable to most reported MOF-coated membranes.[30,31]

The conventional reductive electrosynthesis of HKUST-1 films was conducted with a deposition precursor composed of 50 mM $Cu(NO_3)_2$ and 48 mM H_3BTC and a bare conductive indium tin oxide (ITO) glass as WE (Figure 1a). The electrochemical reactions involved in the MOF generation can be listed as eqs 1−3, with the nitrate anions as pro-bases. It is noteworthy that the coating of metallic Cu (reaction 4) could be favored in the deposition process since the applied potential (−1.6 V vs Ag(cryptand)$^+$/Ag or ~−1.73 V vs SHE) to trigger the deprotonation process (reaction 1) is much negative than the standard potential of Cu^{2+} reduction (+0.34 V vs SHE). Even though the standard electrode potential of reaction 1 is

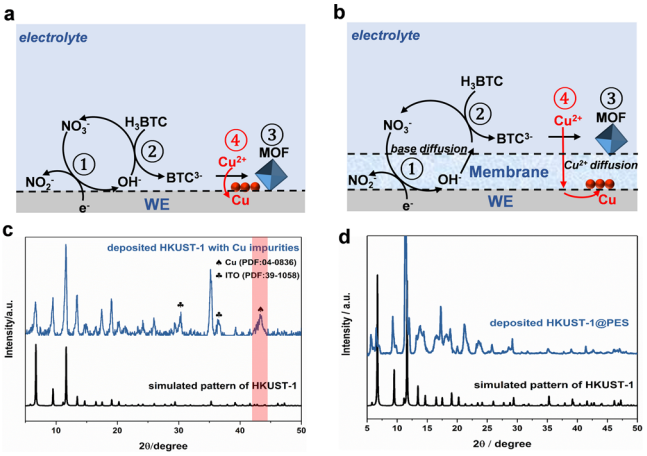

Figure 1. (a) Schematic illustration of the mechanism of conventional reductive synthesis of HKUST-1 films and (c) XRD pattern of the prepared HKUST-1 film by the method. (b) Schematic illustration of the mechanism of proposed modified reductive deposition of HKUST-1 film and (d) XRD pattern of the prepared HKUST-1 film by the method. The dashed lines in panels a and b represent the interfaces.

+0.01 V vs SHE, the practically applied potential should be much more negative than it to ensure a decent deprotonation rate. The coreduction of Cu^{2+} was demonstrated by the cyclic voltammetry (CV) curve recorded in the deposition precursor (Figure S1) which exhibits the typical redox peaks of copper coating and stripping.[32] The presence of metallic Cu was further demonstrated by the XRD pattern of the as-deposited HKUST-1 film on an ITO substrate. As exhibited in Figure 1c, the peaks of metallic Cu and the Cu-MOF were observed, indicating metallic Cu impurities in the HKUST-1 film.

As a comparison, in the modified deposition, the PES membrane is tightly attached to the WE, which creates two interfaces near the WE (WE−membrane interface and membrane−electrolyte interface), as shown in Figure 1b. The homemade deposition setup is shown in Figure S2. The used PES membrane with an asymmetric structure was fabricated by a reported phase inversion approach.[33] The dense part of the membrane is of 2−5 nm pore size. In this configuration, the Cu^{2+} and the nitrate anions with small sizes can easily go through the membrane and reach the conductive WE. In contrast, the linker molecules with larger sizes are less likely to reach the WE−membrane interface with the membrane acting as a barrier for the ion diffusion (see Note S1). Thus, even though the generation of base ions (reaction 1) and the reduction of Cu^{2+} (reaction 4) are conducted at the WE-membrane interface as they behave in the conventional reductive synthesis of HKUST-1, the generated base ions (OH^-) tend to cross the PES membrane and trigger the deprotonation of linkers (reaction 2) on the membrane−electrolyte interface owing to the counter-diffusion effect. As a result, the generation of HKUST-1 film (reaction 3) and the reduction of Cu^{2+} could occur in separate interfaces in this modified deposition, leading to the metallic copper-free HKUST-1 film-coated PES membrane. As displayed in Figure 1d, the XRD pattern of the prepared HKUST-1 film-coated PES membrane via the modified deposition (@-1.73 V vs SHE for 16 h) showed only HKUST-1 peaks after subtracting the signal of the substrate, verifying the coating of pure HKUST-1 film on the PES membrane. It is noteworthy that very few

HKUST-1 crystals were observed on the WE and the backside of the PES membrane because the concentration of the H_3BTC near the WE could be relatively small owing to its large molecular size (the diffusion of the linkers across the membrane is even more difficult when the MOF crystals are formed on the membrane surface).[34] The XRD pattern of the WE after the deposition is shown in Figure S3 in which only the peaks assigned to metallic Cu and ITO were detected. In addition, the PES membrane supported Co-(HBTC)(4,4′-bipy) was also obtained by the modified deposition, indicating the applicability of this method. The XRD pattern and SEM image of the prepared film are displayed in Figures S4 and S5, respectively.

$$NO_3^- + 2e^- + H_2O \rightarrow NO_2^- + 2OH^- \text{ (0.01 V vs SHE)} \quad (1)$$

$$3OH^- + H_3BTC \rightarrow BTC^{3-} + 3H_2O \quad (2)$$

$$2BTC^{3-} + 3Cu^{2+} \rightarrow BTC_2 \text{ (HKUST-1)} \quad (3)$$

$$Cu^{2+} + 2e^- \rightarrow Cu \text{ (0.34 V vs SHE)} \quad (4)$$

To explore the practical uses of the modified reductive deposition, the coatings of HKUST-1 film on the PES membrane with various deposition times (1−20 h) were conducted. According to their optical images shown in Figure S6, the bare PES membrane was gradually covered by the blue HKUST-1 film with the raising of the deposition time. When the coating time was over 16 h, the PES membrane was fully covered by the MOF film. The corresponding top-view and sectional-view SEM images of these prepared samples are displayed in Figures 2 and S7, respectively, in line with the optical observations. When the deposition time was lower than 8 h, the observed HKUST-1 crystals were scattered, and the PES membrane areas could still be seen. As a comparison, the membrane surface was entirely covered with HKUST-1 crystals in the samples with a deposition time larger than 12 h. The formation of a compact HKUST-1 film on the PES membrane can be attributed to the self-closing effect as reported before.[34] Specifically, at the beginning of the deposition, the generated HKUST-1 crystals randomly attach to the PES membrane and act as a barrier to the ions' transfer. Thus, the following generation of HKUST-1 crystals is more likely to occur on the bare PES membrane area until the whole membrane surface is fully covered with MOF crystals. The current−time curve of the modified deposition conducted at −1.73 V vs SHE confirms the self-closing effect, as shown in Figure S8. It can be seen that the current density decreases sharply in the first several hours and then undergoes a slight decrease, which indicates the gradual formation of the compact HKUST-1 film. Notably, when no negative bias is applied to the WE, very few HKUST-1 crystals can be obtained on the PES membrane after 16 h (Figure S9), verifying the proposed deposition method is driven by the negative bias or current.

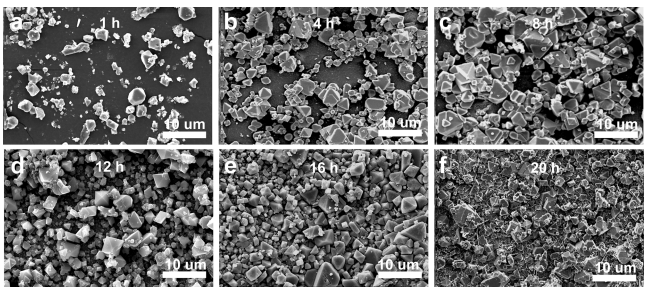

Figure 2. SEM images of the as-prepared HKUST-1@PES films with different deposition times (1−20 h).

The morphology and the thickness of the compact HKUST-1 film supported on the PES membrane after washing away the dangling crystals were examined by scanning electron microscopy. Figure 3a and 3b shows the top view SEM image of the pure PES membrane and the MOF coated membrane, respectively. Unlike the bare surface of the PES membrane shown in Figure 3a, the densely packed octahedral MOF crystals can be clearly seen with the size of several hundreds of nanometers on the as-prepared MOF-covered membrane by the proposed deposition, as displayed in Figure 3b. Also, Figure 3c and 3d show the sectional view SEM image of the PES membrane and the MOF-coated membrane, respectively, validating the successful coating of HKUST-1 film on the PES membrane by the deposition. The thickness of the compact HKUST-1 film can be measured as ∼20 μm. Importantly, no cracks or pinholes were observed from these microscopic images, which guarantees the separation performance of the HKUST-1 covered polymer membrane.

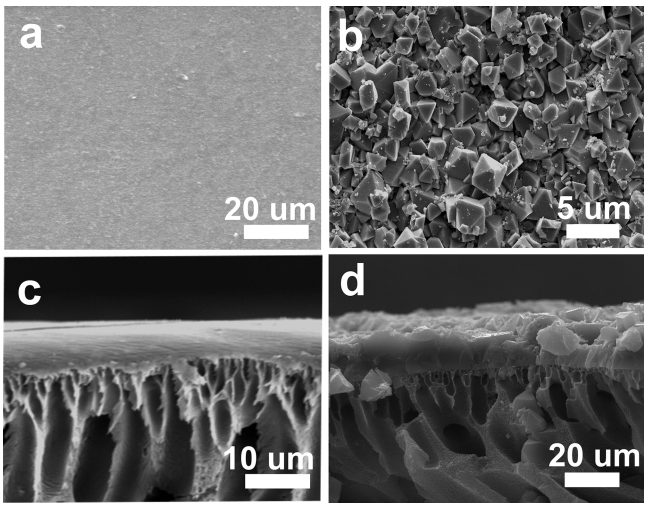

Figure 3. (a) Top view SEM image of PES membrane; (b) top view SEM images of HKUST-1 film-coated PES membrane; (c) sectional view SEM image of PES membrane; and (d) sectional view SEM image of HKUST-1 film-coated PES membrane.

The dye removal performance of the HKUST-1 film-coated PES membranes was examined by a high-throughput filtration setup (Figure S10). The feed-in aqueous solution contained 35 μM rose bengal (M = 1017.64 g mol^{-1}). As shown in Figure 4a, the rejection rate of rose bengal of the HKUST-1 coated PES membranes increases sharply with the deposition time while the permeance behaves the opposite. In particular, the sample with a deposition time of 16 h shows a rejection rate of 98.7% and the corresponding permeance is 7.4 L m^{-2} h^{-1} bar^{-1}, which is comparable to most reported MCPMs (see Table S2). The sample with a deposition time of 20 h even exhibits a slightly higher rejection rate of 98.9% but with a much smaller permeance of 5.2 m^{-2} h^{-1} bar^{-1}. The time-dependent rejection of rose bengal through the HKUST-1 coated PES membrane with 16 h deposition is shown in Figure 4b, which suggests the rejection rate peaks at 20 min and

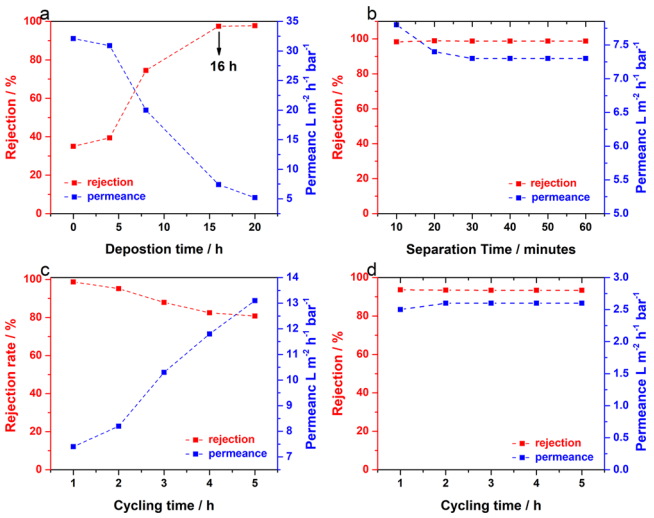

Figure 4. (a) Rose bengal removal performance of HKUST-1 coated PES membranes with various deposition times in an aqueous solution; (b) time-dependent rejection of rose bengal through the HKUST-1 coated PES membrane. Cycling performance for the rose bengal removal in (c) an aqueous solution and (d) an ethanol solution of the HKUST-1 coated PES membrane with 16 h deposition time.

remains in the following 40 min. These results are consistent with the optical and microscopic observations which indicate that the compact HKUST-1 film-covered PES membrane is available in 16 h. Figure 4c displays the stability performance of the sample with 16-h deposition in the dye removal works. It can be seen that the rejection rate of the sample remained >80% of its initial performance after 5 consecutive tests (1 h each), verifying its decent stability in water. The SEM image of the HKUST-1 film after the cycling test in the aqueous solution is shown in Figure S11. It can be seen that the MOF crystals only show a slight degradation which guarantees the decent cycling performance. Notably, the HKUST-1-coated PES membrane showed increased stability in an ethanol solution. The separation performance nearly remains the same after 5 times tests in the ethanol solution, as shown in Figure 4d.

In conclusion, this work proposes a convenient and inexpensive modified reductive electrodeposition method for the preparation of compact HKUST-1 film on polymer (PES) membrane. Taking the advantages of the counter diffusion effect, the proposed deposition method settles the main obstacles remaining in conventional reductive electrosynthesis of MOF films: the codeposition of metallic impurities and the incompatibility of poorly conductive polymer substrates. Specifically, the compact HKUST-1 film can be deposited on the PES membrane in 16 h owing to the self-closing ability of the electrochemical technique by the proposed approach. The HKUST-1 coated PES membrane could be an ideal separation medium for dye-removal which can reject 98.7% of rose bengal from water with a permeance of 7.4 L m^{-2} h^{-1} bar^{-1}, comparable with most reported MOF covered polymer membranes. Future works using the proposed reductive electrodeposition method for the preparation of MCPMs can focus on the following aspects: (1) deposition of chemical stable MOF films like the UiO-66 film and ZIF films, (2) optimizing the deposition parameters to decrease the deposition time, and (3) surface modification of the polymer membrane to deposit oriented MOF films.

Experimental section; CV curve recorded in the deposition electrolyte; schematic diagram of the deposition setup; XRD and SEM characterizations of the deposited Co-MOF; optical and sectional-view SEM images of the deposited HKUST-1 films with different deposition times; chronoamperogram profile of the deposition; optical image of the used separation setup; SEM image of the HKUST-1 film after cycling; comparison of the reported methods and the proposed method for the preparation of MOF films on polymer membrane; and the comparison of the separation performance of the reported MCPMs (PDF)

AUTHOR INFORMATION

Corresponding Authors

Xuan Zhang − *Department of Materials Engineering, KU Leuven, B-3001 Heverlee, Belgium; ZJU-Hangzhou Global Scientific and Technological Innovation Centre, Zhejiang University, Hangzhou 311200, P.R. China;* orcid.org/0000-0002-3667-4280; Email: xuan.zhang@kuleuven.be

Jan Fransaer − *Department of Materials Engineering, KU Leuven, B-3001 Heverlee, Belgium*; Email: jan.franser@kuleuven.be

Authors

Sijie Xie − *Department of Materials Engineering, KU Leuven, B-3001 Heverlee, Belgium*

Xiaoyu Tan − *Centre for Surface Chemistry and Catalysis, KU Leuven, 3001 Leuven, Belgium*

Wei Zhang − *Department of Materials Engineering, KU Leuven, B-3001 Heverlee, Belgium;* orcid.org/0000-0001-7299-6650

Wei Guo − *Department of Materials Engineering, KU Leuven, B-3001 Heverlee, Belgium*

Ning Han − *Department of Materials Engineering, KU Leuven, B-3001 Heverlee, Belgium;* orcid.org/0000-0003-0920-9049

Zhenyu Zhou − *Department of Materials Engineering, KU Leuven, B-3001 Heverlee, Belgium*

Yinzhu Jiang − *ZJU-Hangzhou Global Scientific and Technological Innovation Centre, Zhejiang University, Hangzhou 311200, P.R. China*

Ivo F. J. Vankelecom − *Centre for Surface Chemistry and Catalysis, KU Leuven, 3001 Leuven, Belgium*

Author Contributions

The manuscript was written through contributions of all authors.

Funding

Funding from Research Foundation Flanders (FWO) (12ZV320N) and the National Natural Science Foundation of China (No. 22005250) are acknowledged. S.X., X.T., W.Z.,

and W.G. gratefully acknowledge the China Scholarship Council.

Notes

The authors declare no competing financial interest.

■ ACKNOWLEDGMENTS

The authors also thank Zhenyu Zhao for his assistance with the separation tests and Wouter Monnens for enlightening discussions.

■ REFERENCES

(1) Dolgopolova, E. A.; Rice, A. M.; Martin, C. R.; Shustova, N. B. Photochemistry and photophysics of MOFs: Steps towards MOF-based sensing enhancements. *Chem. Soc. Rev.* **2018**, *47*, 4710−4728.

(2) Ding, M. L.; Flaig, R. W.; Jiang, H. L.; Yaghi, O. M. Carbon capture and conversion using metal−organic frameworks and MOF-based materials. *Chem. Soc. Rev.* **2019**, *48*, 2783−2828.

(3) Jiao, L.; Jiang, H. L. Metal−Organic-Framework-Based Single-Atom Catalysts for Energy Applications. *Chem.* **2019**, *5*, 786−804.

(4) Kang, Y. S.; Lu, Y.; Chen, K.; Zhao, Y.; Wang, P.; Sun, W. Y. Metal−organic frameworks with catalytic centers: From synthesis to catalytic application. *Coord. Chem. Rev.* **2019**, *378*, 262−280.

(5) Xiao, J. D.; Jiang, H. L. Metal−Organic Frameworks for Photocatalysis and Photothermal Catalysis. *Acc. Chem. Res.* **2019**, *52*, 356−366.

(6) Xue, D. X.; Wang, Q.; Bai, J. F. Amide-functionalized metal−organic frameworks: Syntheses, structures and improved gas storage and separation properties. *Coord. Chem. Rev.* **2019**, *378*, 2−16.

(7) Calbo, J.; Golomb, M. J.; Walsh, A. Redox-active metal−organic frameworks for energy conversion and storage. *J. Mater. Chem. A* **2019**, *7*, 16571−16597.

(8) Koo, W. T.; Jang, J. S.; Kim, I. D. Metal-Organic Frameworks for Chemiresistive Sensors. *Chem.* **2019**, *5*, 1938−1963.

(9) Li, W. B. Metal-organic framework membranes: Production, modification, and applications. *Prog. Mater. Sci.* **2019**, *100*, 21−63.

(10) Shekhah, O.; Liu, J.; Fischer, R.; Wöll, C. MOF thin films: existing and future applications. *Chem. Soc. Rev.* **2011**, *40*, 1081−1106.

(11) Denny, M. S.; Moreton, J. C.; Benz, L.; Cohen, S. M. Metal−organic frameworks for membrane-based separations. *Nat. Rev. Mater.* **2016**, *1*, 16078.

(12) Ahmad, M. Z.; Peters, T. A.; Konnertz, N. M.; Visser, T.; Téllez, C.; Coronas, J.; Fila, V.; de Vos, W. M.; Benes, N. E. High-pressure CO_2/CH_4 separation of Zr-MOFs based mixed matrix membranes. *Sep. Purif. Technol.* **2020**, *230*, 115858.

(13) Deng, J.; Dai, Z.; Hou, J.; Deng, L. Morphologically tunable MOF nanosheets in mixed matrix membranes for CO_2 separation. *Chem. Mater.* **2020**, *32*, 4174−4184.

(14) Dechnik, J.; Gascon, J.; Doonan, C. J.; Janiak, C.; Sumby, C. J. Mixed-matrix membranes. *Angew. Chem., Int. Ed.* **2017**, *56*, 9292−9310.

(15) Guo, A.; Ban, Y.; Yang, K.; Yang, W. Metal−organic framework-based mixed matrix membranes: Synergetic effect of adsorption and diffusion for CO_2/CH_4 separation. *J. Membr. Sci.* **2018**, *562*, 76−84.

(16) Zhao, Y.; Wei, Y.; Lyu, L.; Hou, Q.; Caro, J. r.; Wang, H. Flexible polypropylene-supported ZIF-8 membranes for highly efficient propene/propane separation. *J. Am. Chem. Soc.* **2020**, *142*, 20915−20919.

(17) Hou, J.; Sutrisna, P. D.; Zhang, Y.; Chen, V. Formation of ultrathin, continuous metal−organic framework membranes on flexible polymer substrates. *Angew. Chem., Int. Ed.* **2016**, *55*, 3947−3951.

(18) Guo, Y.; Wang, X.; Hu, P.; Peng, X. ZIF-8 coated polyvinylidenefluoride (PVDF) hollow fiber for highly efficient separation of small dye molecules. *Appl. Mater. Today* **2016**, *5*, 103−110.

(19) Shekhah, O.; Wang, H.; Paradinas, M.; Ocal, C.; Schüpbach, B.; Terfort, A.; Zacher, D.; Fischer, R. A.; Wöll, C. Controlling interpenetration in metal−organic frameworks by liquid-phase epitaxy. *Nat. Mater.* **2009**, *8*, 481−484.

(20) Cacho-Bailo, F.; Catalan-Aguirre, S.; Etxeberria-Benavides, M.; Karvan, O.; Sebastian, V.; Tellez, C.; Coronas, J. Metal−organic framework membranes on the inner-side of a polymeric hollow fiber by microfluidic synthesis. *J. Membr. Sci.* **2015**, *476*, 277−285.

(21) Liu, X. L.; Li, Y. S.; Zhu, G. Q.; Ban, Y. J.; Xu, L. Y.; Yang, W. S. An organophilic pervaporation membrane derived from metal−organic framework nanoparticles for efficient recovery of bio-alcohols. *Angew. Chem., Int. Ed.* **2011**, *50*, 10636−10639.

(22) Mintova, S.; Bein, T. Microporous films prepared by spin-coating stable colloidal suspensions of zeolites. *Adv. Mater.* **2001**, *13*, 1880−1883.

(23) Ameloot, R.; Gobechiya, E.; Uji-i, H.; Martens, J. A.; Hofkens, J.; Alaerts, L.; Sels, B. F.; De Vos, D. E. Direct patterning of oriented metal−organic framework crystals via control over crystallization kinetics in clear precursor solutions. *Adv. Mater.* **2010**, *22*, 2685−2688.

(24) Stassen, I.; Styles, M.; Grenci, G.; Van Gorp, H.; Vanderlinden, W.; De Feyter, S.; Falcaro, P.; De Vos, D.; Vereecken, P.; Ameloot, R. Chemical vapour deposition of zeolitic imidazolate framework thin films. *Nat. Mater.* **2016**, *15*, 304−310.

(25) Li, M.; Dincă, M. Reductive electrosynthesis of crystalline metal−organic frameworks. *J. Am. Chem. Soc.* **2011**, *133*, 12926−12929.

(26) Zhang, X.; Wan, K.; Subramanian, P.; Xu, M.; Luo, J.; Fransaer, J. Electrochemical deposition of metal−organic framework films and their applications. *J. Mater. Chem. A* **2020**, *8*, 7569−7587.

(27) Wei, R.; Chi, H. Y.; Li, X.; Lu, D.; Wan, Y.; Yang, C. W.; Lai, Z. Aqueously Cathodic Deposition of ZIF-8 Membranes for Superior Propylene/Propane Separation. *Adv. Funct Mater.* **2020**, *30*, 1907089.

(28) Campagnol, N.; Van Assche, T. R.; Li, M.; Stappers, L.; Dincă, M.; Denayer, J. F.; Binnemans, K.; De Vos, D. E.; Fransaer, J. On the electrochemical deposition of metal−organic frameworks. *J. Mater. Chem. A* **2016**, *4*, 3914−3925.

(29) Xie, S.; Monnens, W.; Wan, K.; Zhang, W.; Guo, W.; Xu, M.; Vankelecom, I. F. J.; Zhang, X.; Fransaer, J. Cathodic Electrodeposition of MOF Films Using Hydrogen Peroxide. *Angew. Chem., Int. Ed.* **2021**, *60*, 24950−24957.

(30) Zhang, C.; Wu, B. H.; Ma, M. Q.; Wang, Z.; Xu, Z. K. Ultrathin metal/covalent−organic framework membranes towards ultimate separation. *Chem. Soc. Rev.* **2019**, *48*, 3811−3841.

(31) Joseph, L.; Jun, B. M.; Jang, M.; Park, C. M.; Munoz-Senmache, J. C.; Hernandez-Maldonado, A. J.; Heyden, A.; Yu, M.; Yoon, Y. Removal of contaminants of emerging concern by metal-organic framework nanoadsorbents: A review. *Chem. Eng. J.* **2019**, *369*, 928−946.

(32) Lane, M.; Murray, C.; McFeely, F.; Vereecken, P.; Rosenberg, R. Liner materials for direct electrodeposition of Cu. *Appl. Phys. Lett.* **2003**, *83*, 2330−2332.

(33) Idris, A.; Mat Zain, N.; Noordin, M.Y. Synthesis, characterization and performance of asymmetric polyethersulfone (PES) ultrafiltration membranes with polyethylene glycol of different molecular weights as additives. *Desalination* **2007**, *207*, 324−339.

(34) Zhang, X.; Li, Y.; Van Goethem, C.; Wan, K.; Zhang, W.; Luo, J.; Vankelecom, I. F.; Fransaer, J. Electrochemically assisted interfacial growth of MOF membranes. *Matter* **2019**, *1*, 1285−1292.